Albedo Observation of C-type Asteroid Ryugu Using the Hayabusa2 LIDAR. R. Yamada[1], H. Araki[2], K. Yamamoto[2], H. Senshu[3], N. Namiki[2], H. Noda[2], K. Matsumoto[2], F. Yoshida[3], S. Abe[4], N. Hirata[1], [1]The University of Aizu (Tsuruga, Ikki-machi, Aizu-wakamatsu, Fukushima, 965-8580, Japan, E-mail: ryamada@u-aizu.ac.jp), [2]National Astronomical Observatory of Japan (2-21-1, Osawa, Mitaka, Tokyo, 181-8588, Japan), [3]Chiba Institute of Technology (2-17-1, Tsudanuma, Narashino,Chiba, 275-0016, Japan), [4]Nihon University (7-24-1, Narashinodai, Funabashi, Chiba, 274-8510, Japan)

Introduction: In June 2018, the Japanese asteroid explorer Hayabusa2 has arrived to C-type asteroid 162173 Ryugu after cruising of about three and half years. The Hayabusa2 has laser altimeter (light detection and ranging: LIDAR) for navigation of the explorer. The main purpose of the LIDAR is to measure the distance between the spacecraft and the asteroid using time delay between the transmission and reception of the laser. In addition, the Hayabusa2 LIDAR has the function of measuring the intensities of a transmitted laser pulse and received laser pulse reflected from the asteroid surface. In this study, we have derived the normal albedo of the Ryugu at the laser wavelength of 1064 nm using the intensity data.

Prior to the Hayabusa2 mission, only closeup exploration has been performed on 253 Mathilde as C-type asteroid by the explorer NEAR Shoemarker [1]. On the Mathilde, the albedo variation on the surface was within $\pm$6% of the mean at wavelength of 550 nm [2]. However, the albedo has been investigated with resolution larger than 500 m per pixel [1], and the observation of normal albedo using the LIDAR has never been performed on C-type asteroid. The size of laser footprint of the Hayabusa2 LIDAR is about 30 m at home position of altitude of 20 km. Our observation will provide first knowledge of normal albedo variation at 1064 nm on C-type asteroid with higher resolution.

Calibration: In the Hayabusa2 LIDAR, the transmitted pulse intensity and the received pulse intensity are recorded as 8-bits digital data of 0-255. We have already derived the method to estimate the normal albedo from the digital data [3]. However, the previous method did not respond to variation of shape of the received pulse due to surface terrain. The received pulse has width of about 10 nsec if the reflecting surface is flat. The pulse width lengthens and the amplitude shrinks if the surface has some slopes and roughness, and the response of the LIDAR receiver would change due to the variation of the pulse change. We have investigated the receiver response to the elongated and shrunk pulse, because the only pulses whose width is about 10 nsec were investigated in previous study [3].

In the investigation, the LIDAR Engineering Model (EM) which has same performance to the LIDAR flight model was used. We prepared four shapes of pulses such as square, gaussian, rising and decreasing pulses output from the pulse generator in the test. Their pulses were input to the LIDAR-EM changing the width (0 – 200 nsec) and amplitude of the pulses (minimum – maximum in the generator), and we have recorded the received pulse intensity to each input pulse.

From results of the experiment, we found that the input pulse energy can be related with received pulse intensity (the observed value) using third polynomial equation regardless of the pulse shape if the pulse width is shorter than 90 nsec. The relation is shown in Fig. 1. In this study, we apply only the pulse shorter than 90 nsec for derivation of normal albedo. We can't relate the received pulse intensity with the energy of pulse whose width is longer than 90 nsec rigidly, and more analysis of the experimental data are required.

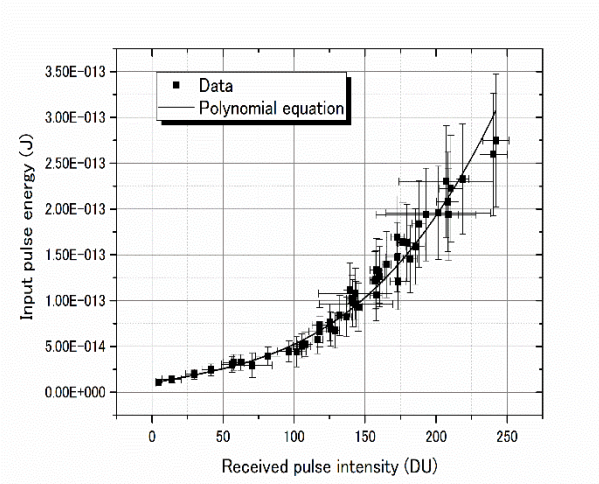

Fig. 1. The relation between the received pulse intensity and the pulse energy. The 51 data are applied to derive the polynomial equation.

Calculation and data selection: The normal albedo ρ on a footprint is calculated using following equation;

$$\rho = (\rho_o * E_{obs})/E_{cal}.$$

The E_{obs} is energy received in the LIDAR receiver, and the value is derived from the observed value (received pulse intensity) using relation shown in Fig. 1. The E_{cal} is the received energy of the calculated pulse reflected from the surface on a footprint. The return pulse is calculated referring method in [4], and the

terrain data on the surface is provided by the Ryugu shape model. In the calculation, some parameters related with characteristics of the LIDAR, the transmitted pulse intensity, and scaling normal albedo ρ_o are applied to simulate the return pulse. Then, we have calculated some types of return pulse using different reflectance models; those are Lambert, Lommel-Seeliger and Oren-Nayer model with some scales of roughness in degrees [5].

For analysis of normal albedo, we have selected the data obtained in 7/20, 8/1,6,7, 9/11,20,21 10/2,3,4, 15,24,31, 11/1, 2018. On the days, the operations in low altitude such as rehearsal of touchdown were performed. We have applied the data obtained at altitude lower than 7 km. In the altitudes, the footprint size is smaller than about 10m and the effect of surface is smaller than that at home position.

Results and Discussion: From the selected data, we could derive the normal albedo around equator of the Ryugu in range of about $\pm$ 20 degrees in latitude using about 375,000 footprints data.

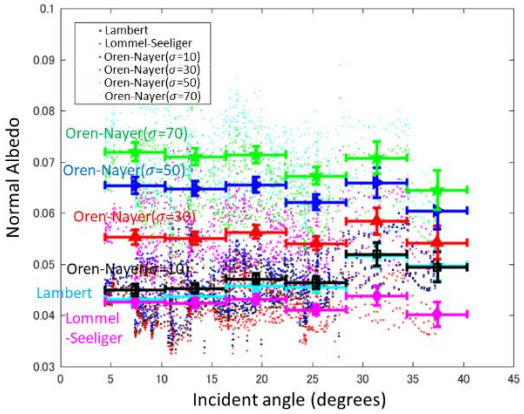

Fig.2 Relation between incident angle and the normal albedo around L08 site for some reflectance models. The small dots represent value of normal albedo of each footprint. The large mark with horizontal and vertical error bars is stacked normal albedo in each angle bin of $\pm$3 degrees.

Fig. 2 shows the estimated normal albedo as function of incident angle around L08 site where is candidate place that the Hayabusa2 will descend for sampling. In the area, there are no distinguish terrains. The all normal albedo are plotted in range of -25~-20 degrees in longitude and 5~10 degrees in latitude in Fig. 2. We found that the values of normal albedo are different for each reflectance model which is used in calculation of return pulse. In Fig. 2, The normal albedo is smallest in Lommel-Seeliger model, and higher in Oren-Nayer model with larger roughness. The values of normal albedo using Lambert model are evidently higher in high incident angle. This is impossible phenomena for real materials as rocks, and we can say that the Lambert model is incorrect to represent reflectance of the area on the Ryugu. In Fig.2, the reflectance model where the normal albedo don't change within the errors for incident angle are Lommel-Seeriger, Oren-Nayer model with roughness from 20 to 50 degrees. If we adopt Oren-Nayer model, range of the normal albedo at 1064nm is in range of 0.05-0.065, and the roughness is in range of 20-50 degrees. On the other hand, if we adopt Lommel-Seeliger model, the normal albedo has values from 0.04-0.045. Using the model, the average in equator area is 0.042, and the deviation is 9.0%. It corresponds to typical albedo of C-type asteroid (0.03-0.06 [6]). The Lommel-Seeliger model is also applied to represent photometric characteristic of the Ryugu observed by ground telescopes [7].

Here, we have to notice that the normal albedo is always measured at phase angle of 0 degree by the LIDAR, and the values include opposition effect. If we compare the normal albedo derived from the LIDAR data and those from other instruments such as optical navigation camera or other studies, the differences of phase angle and wavelength should be considered. Progress of observation and analysis will increase footprint data, and more data in an area reduces error of the normal albedo by the stacking method. Then, we can select appropriate reflectance model with better accuracy. In this presentation, we will also discuss regionality of the normal albedo on Ryugu and the relation with surface terrain.

[1] Ververka J. et al. (1997) *Science*, *278*, 2109–2113. [2] Clark B. E. et al. (1997) *Icarus*, *140*, 53-65. [3] Yamada R. et al. (2017) *Space Sci. Rev.*, *208* 49–64. [4] Lohani B. et al. (2008) *J. Indian Soc. Remote Sens.*, *36(1)*, 1–11. [5] Oren M. and Nayer K. S. (1994) *SIGGRAPH'94*, 239–246. [6] Tedesco E. F. (1992) *Phillips Lab. Tech. Report PL-TR-92-2049*. [7] Lucille L. C. et al. (2018) *MNRAS*, *475*, 614–623.